

Auxin-associated initiation of vascular cell differentiation by LONESOME HIGHWAY

Kyoko Ohashi-Ito^{1,*}, Mio Oguchi¹, Mikiko Kojima², Hitoshi Sakakibara² and Hiroo Fukuda^{1,*}

SUMMARY

Plant vascular tissues are essential for the existence of land plants. Many studies of transcriptional regulation and cell-cell communication have revealed the process underlying the development of vascular tissues from vascular initial cells. However, the initiation of vascular cell differentiation is still a mystery. Here, we report that *LONESOME HIGHWAY* (*LHW*), which encodes a bHLH transcription factor, is expressed in pericycle-vascular mother cells at the globular embryo stage and is required for proper asymmetric cell division to generate vascular initial cells. In addition, ectopic expression of *LHW* elicits an ectopic auxin response. Moreover, *LHW* is required for the correct expression patterns of components related to auxin flow, such as *PIN-FORMED 1* (*PIN1*), *MONOPTEROS* (*MP*) and *ATHB-8*, and *ATHB-8* partially rescues the vascular defects of *lhw*. These results suggest that *LHW* functions as a key regulator to initiate vascular cell differentiation in association with auxin regulation.

KEY WORDS: Auxin, LONESOME HIGHWAY, Root, Vascular development

INTRODUCTION

The vascular bundle is the long-distance transport pathway for water, nutrients and signalling molecules that connect all parts of the plant body. Because the vascular system is an important lifeline, the molecular mechanisms underlying vascular development have been keenly investigated for a long time. Recent genetic and physiological studies have identified many key factors, including transcription factors that govern vascular development, suggesting the importance of transcriptional regulation in the developmental process, especially during differentiation of specialized vascular cells (Caño-Delgado et al., 2010; Ohashi-Ito and Fukuda, 2010; Scarpella and Helariutta, 2010). By contrast, the mode of transcriptional regulation of the initiation of vascular initial cells is largely unknown.

We recently identified *LONESOME HIGHWAY* (*LHW*), which encodes a bHLH transcription factor. Mutations of this gene eliminate the bilateral symmetry of the vascular pattern and reduce the number of cells in root vasculatures, resulting in roots with the monoarch vasculature that contains only single xylem and phloem poles (Ohashi-Ito and Bergmann, 2007; Parizot et al., 2008). The *lhw* mutant also shows a weak auxin-related phenotype. Polar auxin flow mediated by auxin efflux carriers has been implicated as the earliest event in vascular differentiation (Scarpella et al., 2006; Donner et al., 2009; Wenzel et al., 2007). In this study, therefore, we investigated the role of *LHW* in the initiation of vascular formation, focusing on the association of *LHW* with the regulation of auxin flow.

MATERIALS AND METHODS

Growth conditions for *Arabidopsis*

A. thaliana ecotype Columbia was used for all experiments. Seedlings were germinated on half-strength MS agar plates and were cultured vertically in a Percival incubator under 24-hour light for 5 to 7 days at 22°C. For *LHW* induction, 7-day-old seedlings grown on MS plates were moved into liquid

MS with or without 5 µM estrogen and incubated with rotation. For the NPA (1-N-Naphthylphthalamic acid)-treatment experiment, 10 µM NPA was added to liquid MS and incubated for 24 hours.

Whole-mount *in situ* hybridization

Whole-mount *in situ* hybridization was performed according to a previously described method (Hejátko et al., 2006).

Histology

Sections of 1.5 µm were prepared as previously described (Hirakawa et al., 2010). Specimens were observed under a DIC microscope with a Charge-Coupled Device camera (BX51, DB70, Olympus, Tokyo, Japan).

Imaging

Fluorescent images were taken using previously described units (Kondo et al., 2011). Images were digitally analyzed using ImageJ. For staining of the plasma membrane, roots were incubated in 0.01 mg/ml propidium iodide. Three-dimensional images were constructed using the interactive 3D surface-plotting tool in ImageJ.

Quantitative RT-PCR

Quantitative RT-PCR was performed according to previously described methods (Ohashi-Ito et al., 2010).

Cloning

Vectors based on Gateway cloning technology (Invitrogen) were used for most manipulations. Promoter fragments were introduced into pBGYN (Kubo et al., 2005). To generate an estradiol-inducible *LHW*, the *LHW*-coding sequence was recombined with pMDC7 (Curtis and Grossniklaus, 2003). To produce *SHR::ATHB-8⁺* and *SHR::PHB⁺*, the 2.0 kb *SHR* promoter was ligated into the *NotI* sites within pENTR/D/TOPO immediately upstream of *ATHB-8⁺* or *PHB⁺*. Primers are listed in supplementary material Table S1.

Quantification of endogenous hormone levels

Roots of 5-day-old seedlings (~20 mg FW) were used for the quantification, which was performed according to Kojima et al. (Kojima et al., 2009).

RESULTS AND DISCUSSION

The defect of bilateral pattern formation in the vasculature of *lhw* roots occurred during early embryogenesis

The vasculatures of wild-type *Arabidopsis* roots contain two protoxylem cells and two protophloem cells that are arranged in

¹Department of Biological Sciences, Graduate School of Science, The University of Tokyo, 7-3-1 Hongo, Bunkyo-ku, Tokyo, 113-0033, Japan. ²RIKEN Plant Science Center, 1-7-22 Suehiro, Tsurumi, Yokohama, 230-0045, Japan.

* Authors for correspondence (kyoko@biol.s.u-tokyo.ac.jp; fukuda@biol.s.u-tokyo.ac.jp)

bilateral symmetry. The *lhw* mutants fail to form the correct vascular pattern and lack bilateral symmetry in the vasculature of seedling roots. To uncover the origin of this defect, we first investigated *LHW* expression during embryogenesis using whole-mount in situ hybridization. The signal from *LHW* was first observed in globular-stage embryos, where it was restricted to the central cells (pericycle-vascular mother cells) that are destined to divide to produce vascular initial cells (Fig. 1A,B). After the heart stage, the *LHW* transcript accumulated in root vascular cells, especially near the root apical meristem (Fig. 1C-E).

Because *LHW* was expressed preferentially in pericycle-vascular mother cells during embryogenesis, we postulated that *LHW* controls the vascular patterning in embryos. To examine this possibility, we observed expression patterns of *TARGET OF MONOPTEROS5* (*TMO5*) and *TMO5-LIKE1* genes as pre-protaxylem markers in embryos. *TMO5* and *TMO5-LIKE1* signals formed two stripes in the provascular region of wild-type embryos after the early heart stage of development (Fig. 1F-I; supplementary material Fig. S1A-C), indicating that the pre-pattern of bilateral symmetry of vasculature is established as early as the heart stage during embryogenesis.

In *lhw* embryos, however, the signals from *TMO5* and *TMO5-LIKE1* were detected as a single stripe in the provascular region throughout embryogenesis (Fig. 1J-L; supplementary material Fig. S1D-F). These results indicate that the bilateral pattern of vasculature is already impaired in early embryos, and that the defect in the *lhw* mutant can be traced back to the early stage embryo.

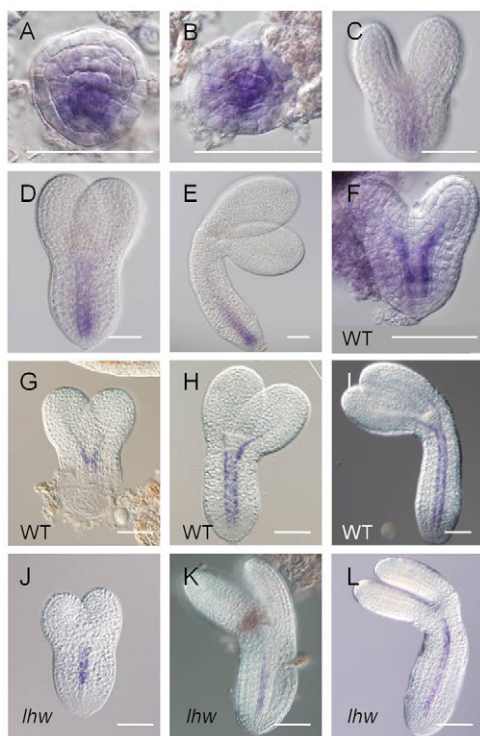


Fig. 1. *LHW* regulates bilateral symmetry in vasculature during embryogenesis. (A-E) Accumulation of *LHW* transcripts in globular stage embryos observed longitudinally (A) and transversely (B) in heart stage embryos (C), in a torpedo stage embryo (D) and in a bent cotyledon stage embryo (E). (F-L) Accumulation of *TMO5* transcripts. Wild-type embryos (F-I) and *lhw* mutant embryos (J-L). Scale bars: 50 μ m.

LHW regulates the first step of vascular initial cell formation

To investigate the *LHW* function in early embryogenesis, we next analyzed the cell division pattern during early development of wild-type and *lhw* embryos in detail, with a special focus on vascular initial cell formation. Wild-type and *lhw* embryos at the globular stage showed very similar cell division patterns in all cells (supplementary material Fig. S2A-D). In wild-type embryos at the transition stage, four vascular initial cells were formed from four pericycle-vascular mother cells by asymmetric cell division (Fig. 2A; supplementary material Fig. S2E,F). Because all vascular cells, not including pericycle cells, are derived from these newly produced four cells, we defined these cells as vascular initial cells. In *lhw* embryos, however, the direction of division in pericycle-vascular mother cells was abnormal, although the division patterns of protodermal and ground cells were not different from those of the wild type (Fig. 2B; supplementary material Fig. S2G,H). As a result, *lhw* embryos possessed fewer vascular initial cells (3 ± 0.37)

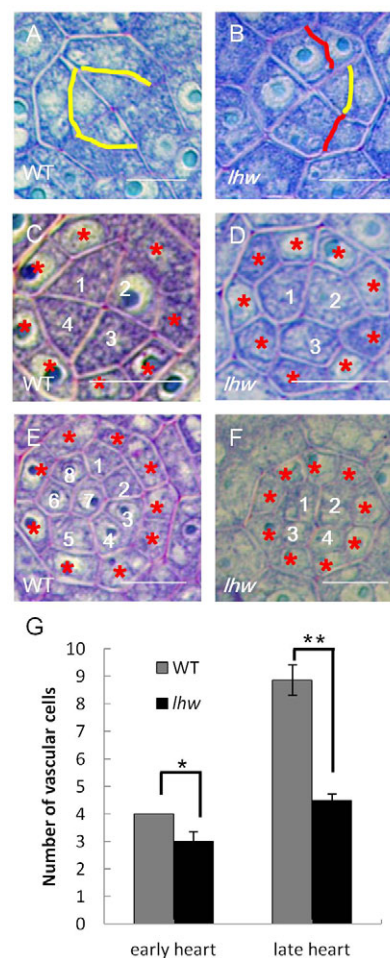


Fig. 2. *LHW* regulates vascular initial cell formation. Anatomical analysis of the central regions of embryos. (A,B) Transition stage embryos of wild type (A) and *lhw* (B). The yellow lines indicate a normal plane of cell division to create a vascular initial cell. The red lines indicate an abnormal plane of cell division. (C,D) Early heart stage embryos of wild type (C) and *lhw* (D). (E,F) Late heart stage embryos of wild type (E) and *lhw* (F). Stars indicate pericycle cells. Each cell is numbered. (G) The number of vascular cells in early heart and late heart stages embryos of wild type (gray) and *lhw* (black). Bars indicate s.d. $n > 6$, * $P < 0.05$, ** $P < 0.01$ (t-test). Scale bars: 10 μ m.

and irregularly shaped cells in the center, whereas wild-type embryos had four uniform vascular initial cells (Fig. 2C,D,G). At the late heart stage, the number of vascular cells was 8.85 ± 0.55 in the wild type but only 4.5 ± 0.22 in *lhw*, indicating that the vascular initial cells in *lhw* embryos rarely divided (Fig. 2E-G). These results suggest that LHW plays a role in the establishment of vascular initial cells during early embryo development through the regulation of cell division, and the monoarch pattern in *lhw* may result from the reduced number of vascular cells, which are insufficient for creating the diarch pattern during the heart stage of embryogenesis.

The expressing region of *PIN1*

Because the early vascular development is associated with auxin flow, the expression pattern of an auxin efflux carrier, *PIN1::PIN1-GFP*, was examined in wild-type and *lhw* embryos (Gälweiler et al., 1998; Friml et al., 2003). It was difficult to find a difference in *PIN1* expression between these embryos before the transition stage (supplementary material Fig. S3). During the early heart stage, *PIN1* expression was restricted in two cotyledon primordia and provascular cells in wild-type embryos (Fig. 3A,C). At this stage, in *lhw* embryos, although the general pattern of *PIN1* expression was similar to that of wild type, the *PIN1*-expressing domain was enlarged (Fig. 3B,D). The enlarged *PIN1* expression was observed in cotyledon primordia where *LHW* was not expressed, suggesting non cell-autonomous effects of LHW. Altered *PIN1* expression was also observed during provascular tissue formation in lateral root primordia. The *PIN1* expression domain in lateral root primordia was gradually restricted to the provascular region and the root tip in wild type (Fig. 3E-G), whereas it was diffused more broadly and expanded to the cortex, endodermis and epidermal cells in *lhw* (Fig. 3I-K). To quantify the changes of the *PIN1*-expressing domain, we also observed the expression pattern of the *PIN1::YFP-nuclear localization signal* (nls) in wild-type and *lhw* lateral root primordia (Fig. 3H,L). The relative signal intensity of the central region (provascular region) to that of the peripheral region of wild-type primordia was considerably higher than was the case for *lhw* primordia (Fig. 3S). These results suggest that the restricted flow of auxin into the future provascular region may not be established in *lhw*.

To investigate whether the broad *PIN1* expression domain in *lhw* is associated with changes in auxin distribution, we next examined *DR5::GFP* expression as a marker of the auxin maximum (Benková et al., 2003). Although *DR5* expression was concentrated to the central region of the meristem in the emerging wild-type lateral root primordia, the peak of *DR5* signal in *lhw* primordia was not restricted to the central region (Fig. 3M-R). These results indicate that the *lhw* plant fails to form a proper *PIN1* expression domain and the proper auxin maximum in the central region of the primordium.

LHW induces the auxin response

To further elucidate how the function of *LHW* relates to auxin flow, we analyzed the auxin response in roots of *LHW* gain-of-function seedlings using *DR5::GFP*, in which *LHW* expression was temporally induced by the addition of estrogen. The addition of estrogen induced the overproduction of the *LHW* transcript (supplementary material Fig. S4A). Without the addition of estrogen, *DR5::GFP* was detected only in the stele and root tip (Fig. 4A; supplementary material Fig. S5A). The addition of estrogen caused ectopic *DR5::GFP* expression in the entire root, which contained the cortex, the endodermis and the epidermis, as

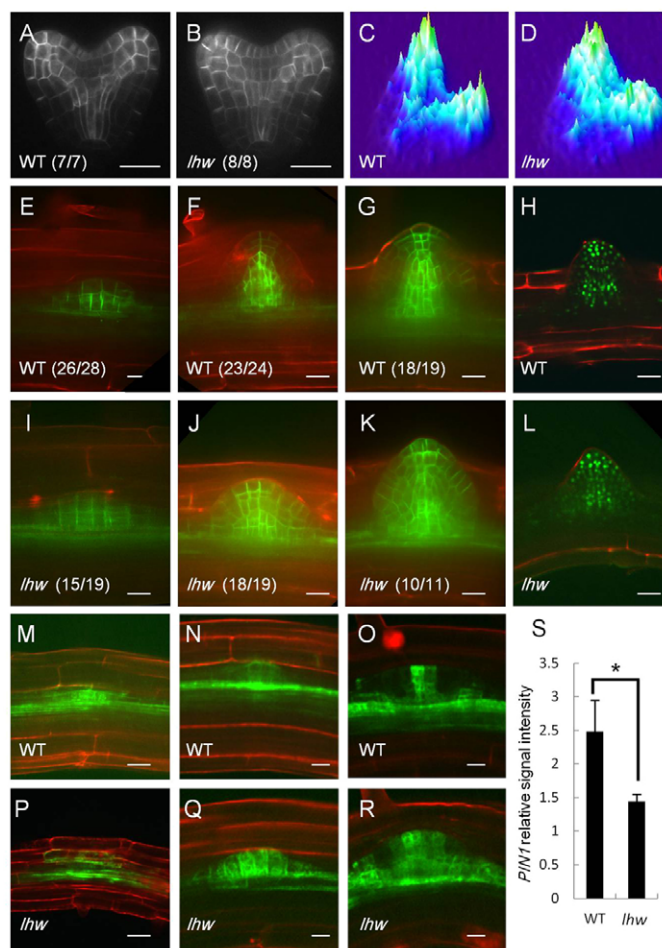


Fig. 3. LHW regulates the establishment of the correct *PIN1* expression pattern and the auxin maximum. (A,B) *PIN1::PIN1-GFP* expression in heart stage embryos of wild type (A) and *lhw* (B). (C,D) 3D images displaying signal intensities of A and B, respectively. (E-G,I-K) *PIN1::PIN1-GFP* expression patterns in lateral root primordia of wild type (E-G) and *lhw* (I-K). Fraction of samples showing a similar pattern are shown in the image. (H,L) *PIN1::YFP-nls* expression images in lateral root primordia of wild type (H) and *lhw* (L). (M-R) *DR5::GFP* expression patterns in lateral root primordia of wild type (M-O) and *lhw* (P-R). (S) Relative *PIN1::YFP-nls* signal intensity in stele region versus ground tissue region. Bars indicate s.d. $n=5$, $*P<0.01$ (t-test). Scale bars: 20 μ m.

well as the stele, within 6 hours (Fig. 4B). Twenty four hours after the addition of estrogen, an ectopic, strong *DR5* signal was maintained in the entire root (Fig. 4D; supplementary material Fig. S4B). These results suggest that ectopic *LHW* induces ectopic auxin response. Although NPA treatment altered the *DR5::GFP* expression pattern in root tips (supplementary material Fig. S5A-D), the treatment did not interfere with the ectopic expression of *DR5::GFP* in *LHW*-overexpressing roots (supplementary material Fig. S5E-G). Therefore, LHW may not promote *DR5* expression by the inhibition of auxin transport through efflux transporters.

Next, to determine whether LHW promotes auxin biosynthesis, we quantified endogenous phytohormone levels, including auxin levels, in the roots of wild type and *lhw* and in roots in which *LHW* was induced for 6 hours and 24 hours (supplementary material Table S2). The free IAA level did not change in these roots (supplementary material Fig. S6). These results suggest that ectopic

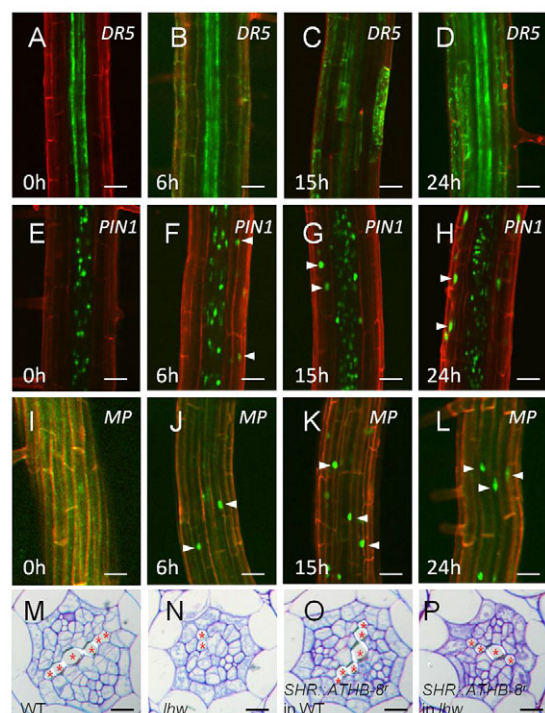


Fig. 4. LHW induces the auxin response. (A–L) Changes in *DR5::GFP* (A–D), *PIN1::YFP-nls* (E–H) and *MP::YFP-nls* (I–L) signals in estrogen-inducible *LHW* plants. Images were taken 0 hours (A,E,I), 6 hours (B,F,J), 15 hours (C,G,K) and 24 hours (D,H,L) after the addition of estrogen. Arrowheads indicate ectopic signals that emerged after *LHW* induction. Images of *MP::YFP-nls* were taken with a focus on the root surface to emphasize ectopic signals. Scale bars: 50 μ m. (M–P) Root sections of wild type (M), *lhw* (N), *SHR::ATHB-8* in wild type (O) and *SHR::ATHB-8* in *lhw* (P). Stars indicate xylem vessel cells. Scale bars: 10 μ m.

DR5 expression caused by *LHW* overexpression may not result from ectopic auxin biosynthesis. Similarly, there were no significant differences in the levels of other hormones in the roots of wild-type, *lhw* or *LHW*-induced plants (supplementary material Table S2).

LHW modulates the auxin signalling

To further understand the role of *LHW* in vascular differentiation in relation to auxin, we examined the involvement of *LHW* in the expression of transcription factors regulating auxin signalling in vasculature. *MP* and *ATHB-8* are transcription factors that are involved in auxin signalling, and they are expressed in the provascular region (Hardtke and Berleth, 1998; Donner et al., 2009; Baima et al., 1995; Ohashi-Ito and Fukuda, 2010). First, we analyzed expression patterns of *MP* and *ATHB-8*. The *MP* signal was observed in the provascular region in wild-type heart stage embryos, as expected (supplementary material Fig. S7A). In *lhw* embryos, the *MP* signal was much weaker than that in the wild-type, especially in the provascular region (supplementary material Fig. S7B). The *ATHB-8* signal was also weaker in *lhw* embryos (supplementary material Fig. S8A,B). To confirm the reduction of *MP* expression in the provascular region in *lhw*, the expression of *MP::YFP-nls* was examined in the lateral root primordia and main roots of seedlings. Indeed, the *MP* signals in the vasculature were diminished in both root primordia and the main root of *lhw* (supplementary material Fig. S7C–G).

Quantitative PCR indicated that the transcript levels of *MP* and *ATHB-8* were lower in *lhw* roots than in wild-type roots (supplementary material Fig. S8C). These results clearly indicate that *LHW* is required for promoting the expression of *MP* and *ATHB-8* in the provascular region.

Next, we analyzed the effects of *LHW* induction on *MP* and *PIN1* expression. Because the ectopic *DR5::GFP* signal was clearly seen 6 hours after *LHW* induction, followed by an increase until 24 hours after induction (Fig. 4B–D), we observed the expression patterns of *MP::YFP-nls* and *PIN1::YFP-nls* at the same time points after *LHW* induction. Ectopic signals of *MP::YFP-nls* and *PIN1::YFP-nls* were indeed seen 6 hours after *LHW* induction, after which time the signals gradually increased (Fig. 4E–L).

To clarify whether *LHW* regulates auxin signalling via *ATHB-8*, we examined the genetic interaction between *lhw* and a gain-of-function mutant of *ATHB-8*. Because *ATHB-8* mRNA levels are repressed by miR165/166, we introduced substitutions into the *ATHB-8* sequence to produce a mutant that was resistant to miR165/166 without introducing amino acid changes (*ATHB-8*^r) (Mallory et al., 2004; Emery et al., 2003). We also employed the *SHR* promoter to continuously overexpress *ATHB-8*^r in provascular tissues because *SHR* is specifically expressed in the provascular region from the late globular stage of embryos (Helariutta et al., 2000). *SHR::PHABULOSA*^r (*PHB*^r), which is another HD-ZIP III transcription factor but is not induced by auxin, was used as a control. The introduction of *SHR::PHB*^r into *lhw* plants did not alter the monoarch vascular pattern in *lhw* roots (supplementary material Fig. S8E). By contrast, *SHR::ATHB-8*^r rescued the *lhw* phenotype and produced the bilateral symmetry pattern in the vasculature of roots, although the rescue of this phenotype was only partial (9/34 plants, Fig. 4M–P; supplementary material Fig. S8D). These data strongly suggest that *LHW* functions in early vascular pattern determination through the enhanced expression of *ATHB-8*.

Our results suggest that *LHW* functions as a key regulator to generate vascular initial cells. In addition, they also suggest that the *LHW* function is closely related to the modulation of auxin response. Although how *LHW* is connected to the auxin response remains obscure, several possibilities are considered. Our favorite hypothesis is that *LHW* may be the first factor to initiate the auxin response by inducing auxin canalization. According to this hypothesis, *LHW* is expressed and induces the auxin response in the future vascular region, and then this restricted auxin response enhances the auxin positive-feedback loops consisting of *PIN1*, *MP* and *ATHB-8*, followed by auxin canalization, which in turn initiates vascular development (Scarpella et al., 2006; Wenzel et al., 2007; Donner et al., 2009; Ohashi-Ito and Fukuda, 2010). Another possible hypothesis is that *LHW* directly regulates auxin signalling components such as *MP* and *ATHB-8* or regulators that modulate the *PIN1* localization. It is well known that cytokinin, along with auxin, regulates vascular pattern formation (Bishopp et al., 2011a; Bishopp et al., 2011b; Cui et al., 2011). Therefore, we cannot deny the possibility that *LHW* induces the auxin response by modulating cytokinin signalling. Further investigation of the target genes of *LHW* may lead to an answer to the relationship between *LHW* and auxin.

Acknowledgements

We thank Minobu Shimizu, Sumika Tsuji-Tsukinoki and Kuninori Iwamoto for technical support; Shigeyuki Betsuyaku for assistance with the whole-mount *in situ* hybridization experiment; Dominique Bergmann and Jiri Friml for seeds; and Nam-Hai Chua for the pMDC7 vector.

Funding

This work was supported in part by the Japan Society for the Promotion of Science (JSPS) [KAKENHI 23227001 and 19060009] and by the NC-CARP project from the Ministry of Education, Culture, Sports, Science and Technology (MEXT).

Competing interests statement

The authors declare no competing financial interests.

Supplementary material

Supplementary material available online at

<http://dev.biologists.org/lookup/suppl/doi:10.1242/dev.087924/-/DC1>

References

- Baima, S., Nobili, F., Sessa, G., Lucchetti, S., Ruberti, I. and Morelli, G. (1995). The expression of the *Athb-8* homeobox gene is restricted to provascular cells in *Arabidopsis thaliana*. *Development* **121**, 4171-4182.
- Benková, E., Michniewicz, M., Sauer, M., Teichmann, T., Seifertová, D., Jürgens, G. and Friml, J. (2003). Local, efflux-dependent auxin gradients as a common module for plant organ formation. *Cell* **115**, 591-602.
- Bishopp, A., Help, H., El-Showk, S., Weijers, D., Scheres, B., Friml, J., Benková, E., Mähönen, A. P. and Helariutta, Y. (2011a). A mutually inhibitory interaction between auxin and cytokinin specifies vascular pattern in roots. *Curr. Biol.* **21**, 917-926.
- Bishopp, A., Lehesranta, S., Vátén, A., Help, H., El-Showk, S., Scheres, B., Helariutta, K., Mähönen, A. P., Sakakibara, H. and Helariutta, Y. (2011b). Phloem-transported cytokinin regulates polar auxin transport and maintains vascular pattern in the root meristem. *Curr. Biol.* **21**, 927-932.
- Caño-Delgado, A., Lee, J. Y. and Demura, T. (2010). Regulatory mechanisms for specification and patterning of plant vascular tissues. *Annu. Rev. Cell Dev. Biol.* **26**, 605-637.
- Cui, H., Hao, Y., Kovtun, M., Stolz, V., Deng, X. W., Sakakibara, H. and Kojima, M. (2011). Genome-wide direct target analysis reveals a role for *SHORT-ROOT* in root vascular patterning through cytokinin homeostasis. *Plant Physiol.* **157**, 1221-1231.
- Curtis, M. D. and Grossniklaus, U. (2003). A gateway cloning vector set for high-throughput functional analysis of genes in planta. *Plant Physiol.* **133**, 462-469.
- Donner, T. J., Sherr, I. and Scarpella, E. (2009). Regulation of preprocambial cell state acquisition by auxin signaling in *Arabidopsis* leaves. *Development* **136**, 3235-3246.
- Emery, J. F., Floyd, S. K., Alvarez, J., Eshed, Y., Hawker, N. P., Izhaki, A., Baum, S. F. and Bowman, J. L. (2003). Radial patterning of *Arabidopsis* shoots by class III HD-ZIP and KANADI genes. *Curr. Biol.* **13**, 1768-1774.
- Friml, J., Vieten, A., Sauer, M., Weijers, D., Schwarz, H., Hamann, T., Offringa, R. and Jürgens, G. (2003). Efflux-dependent auxin gradients establish the apical-basal axis of *Arabidopsis*. *Nature* **426**, 147-153.
- Gälweiler, L., Guan, C., Müller, A., Wisman, E., Mendgen, K., Yephremov, A. and Palme, K. (1998). Regulation of polar auxin transport by AtPIN1 in *Arabidopsis* vascular tissue. *Science* **282**, 2226-2230.
- Hardtke, C. S. and Berleth, T. (1998). The *Arabidopsis* gene *MONOPTEROS* encodes a transcription factor mediating embryo axis formation and vascular development. *EMBO J.* **17**, 1405-1411.
- Hejático, J., Blilou, I., Brewer, P. B., Friml, J., Scheres, B. and Benková, E. (2006). In situ hybridization technique for mRNA detection in whole mount *Arabidopsis* samples. *Nat. Protoc.* **1**, 1939-1946.
- Helariutta, Y., Fukaki, H., Wysocka-Diller, J., Nakajima, K., Jung, J., Sena, G., Hauser, M. T. and Benfey, P. N. (2000). The *SHORT-ROOT* gene controls radial patterning of the *Arabidopsis* root through radial signaling. *Cell* **101**, 555-567.
- Hirakawa, Y., Kondo, Y. and Fukuda, H. (2010). TDF peptide signaling regulates vascular stem cell proliferation via the *WOX4* homeobox gene in *Arabidopsis*. *Plant Cell* **22**, 2618-2629.
- Kojima, M., Kamada-Nobusada, T., Komatsu, H., Takei, K., Kuroha, T., Mizutani, M., Ashikari, M., Ueguchi-Tanaka, M., Matsuoka, M., Suzuki, K. et al. (2009). Highly sensitive and high-throughput analysis of plant hormones using MS-probe modification and liquid chromatography-tandem mass spectrometry: an application for hormone profiling in *Oryza sativa*. *Plant Cell Physiol.* **50**, 1201-1214.
- Kondo, Y., Hirakawa, Y., Kieber, J. J. and Fukuda, H. (2011). CLE peptides can negatively regulate protoxylem vessel formation via cytokinin signaling. *Plant Cell Physiol.* **52**, 37-48.
- Kubo, M., Udagawa, M., Nishikubo, N., Horiguchi, G., Yamaguchi, M., Ito, J., Mimura, T., Fukuda, H. and Demura, T. (2005). Transcription switches for protoxylem and metaxylem vessel formation. *Genes Dev.* **19**, 1855-1860.
- Mallory, A. C., Reinhart, B. J., Jones-Rhoades, M. W., Tang, G., Zamore, P. D., Barton, M. K. and Bartel, D. P. (2004). MicroRNA control of *PHABULOSA* in leaf development: importance of pairing to the microRNA 5' region. *EMBO J.* **23**, 3356-3364.
- Ohashi-Ito, K. and Bergmann, D. C. (2007). Regulation of the *Arabidopsis* root vascular initial population by *LONESOME HIGHWAY*. *Development* **134**, 2959-2968.
- Ohashi-Ito, K. and Fukuda, H. (2010). Transcriptional regulation of vascular cell fates. *Curr. Opin. Plant Biol.* **13**, 670-676.
- Ohashi-Ito, K., Oda, Y. and Fukuda, H. (2010). *Arabidopsis* *VASCULAR-RELATED NAC-DOMAIN6* directly regulates the genes that govern programmed cell death and secondary wall formation during xylem differentiation. *Plant Cell* **22**, 3461-3473.
- Parizot, B., Laplace, L., Ricaud, L., Boucheron-Dubuisson, E., Bayle, V., Bonke, M., De Smet, I., Poethig, S. R., Helariutta, Y., Haseloff, J. et al. (2008). Diarch symmetry of the vascular bundle in *Arabidopsis* root encompasses the pericycle and is reflected in distich lateral root initiation. *Plant Physiol.* **146**, 140-148.
- Scarpella, E. and Helariutta, Y. (2010). Vascular pattern formation in plants. *Curr. Top. Dev. Biol.* **91**, 221-265.
- Scarpella, E., Marcos, D., Friml, J. and Berleth, T. (2006). Control of leaf vascular patterning by polar auxin transport. *Genes Dev.* **20**, 1015-1027.
- Wenzel, C. L., Schuetz, M., Yu, Q. and Mattsson, J. (2007). Dynamics of *MONOPTEROS* and *PIN-FORMED1* expression during leaf vein pattern formation in *Arabidopsis thaliana*. *Plant J.* **49**, 387-398.

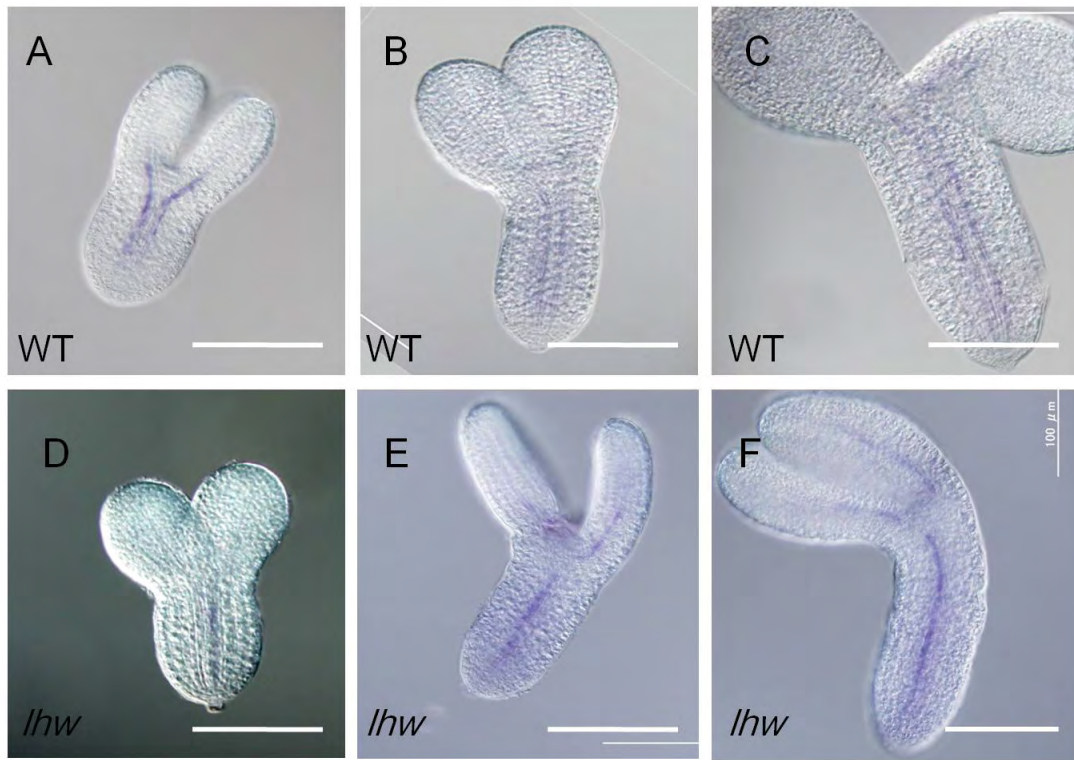


Fig. S1. Accumulation of *TMO5-LIKE1* transcripts during embryogenesis of *Arabidopsis*. (A-F) Accumulation of *TMO5-LIKE1* transcripts in wild-type embryos (A-C) and *lhw* mutant embryos (D-F). Scale bars: 50 μ m.

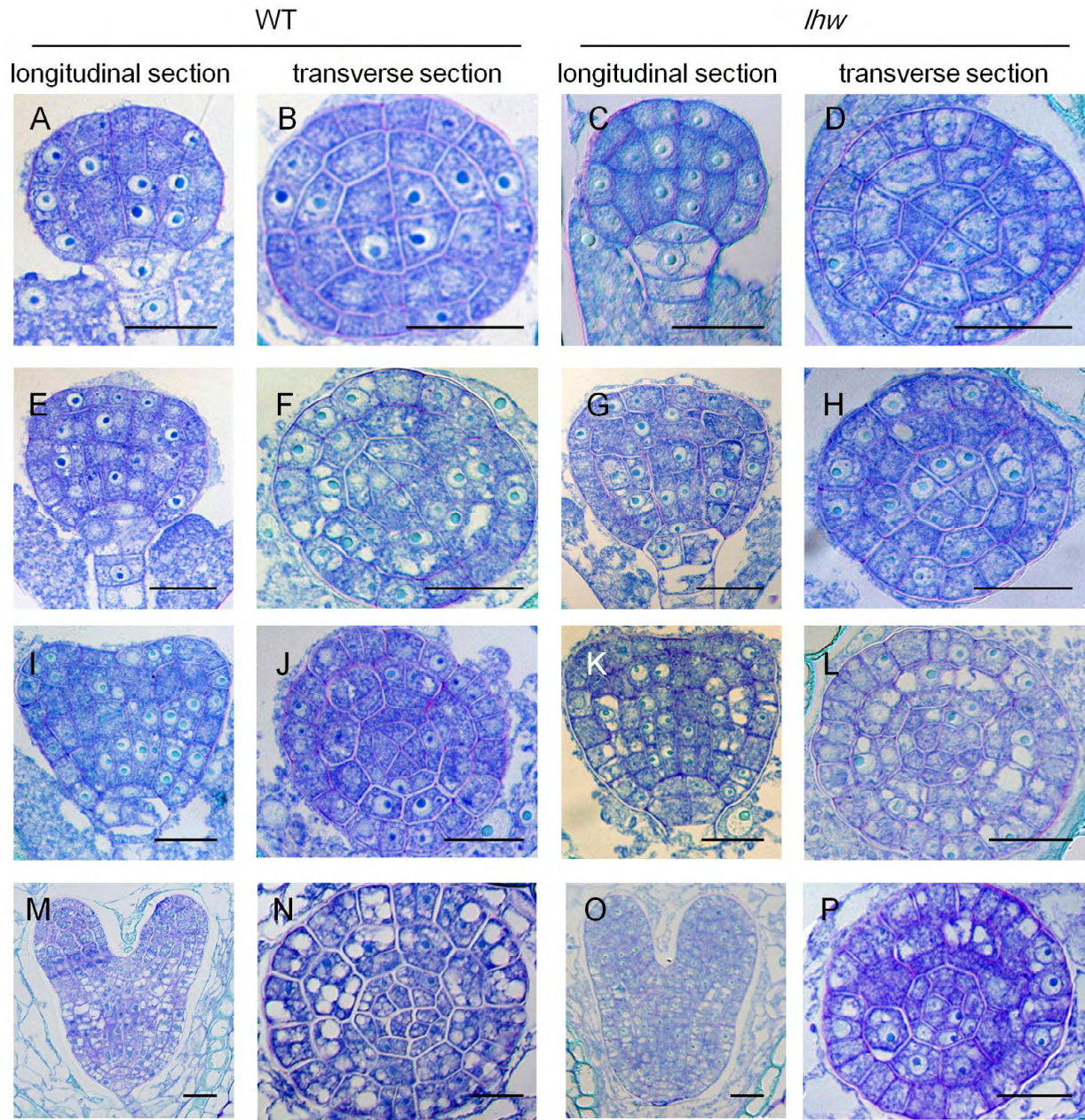


Fig. S2. Anatomical analysis of wild-type and *lhw* embryos. (A-D) Globular-stage embryos of wild type (A,B) and *lhw* (C,D). (E-H) Transition stage embryos of wild-type (E,F) and *lhw* (G,H). (I-L) Early heart stage embryos of wild type (I,J) and *lhw* (K,L). (M-P) Late heart stage embryos of wild type (M,N) and *lhw* (O,P). Scale bars: 20 μ m.

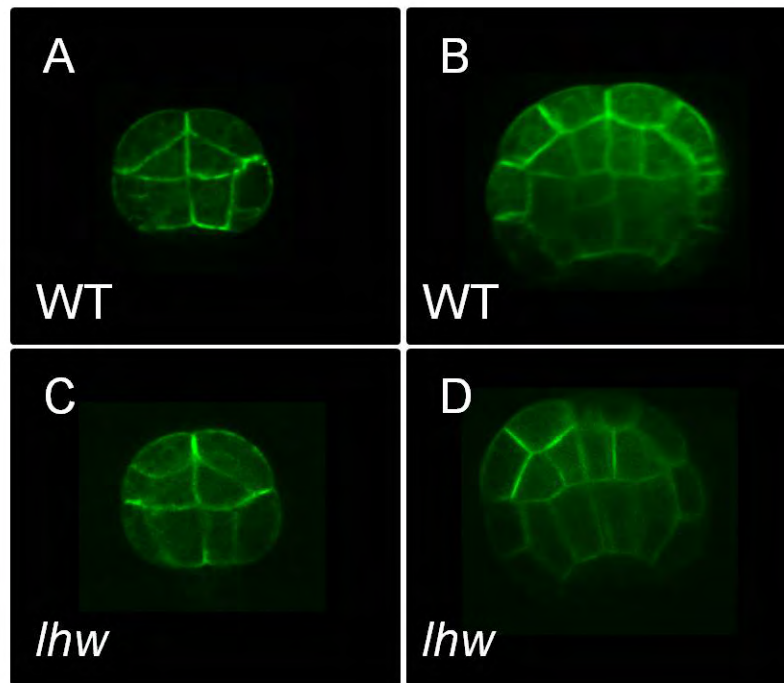


Fig. S3. Expression patterns of *PIN1::PIN1-GFP* during early embryogenesis. (A,B) Wild-type embryos; (C,D) *lhw* embryos.

A

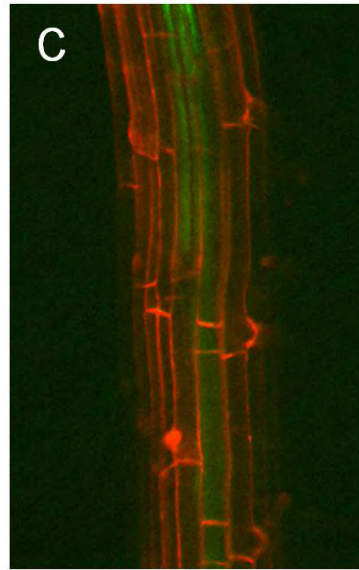
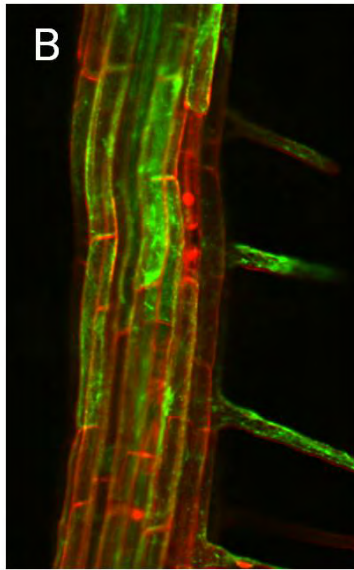
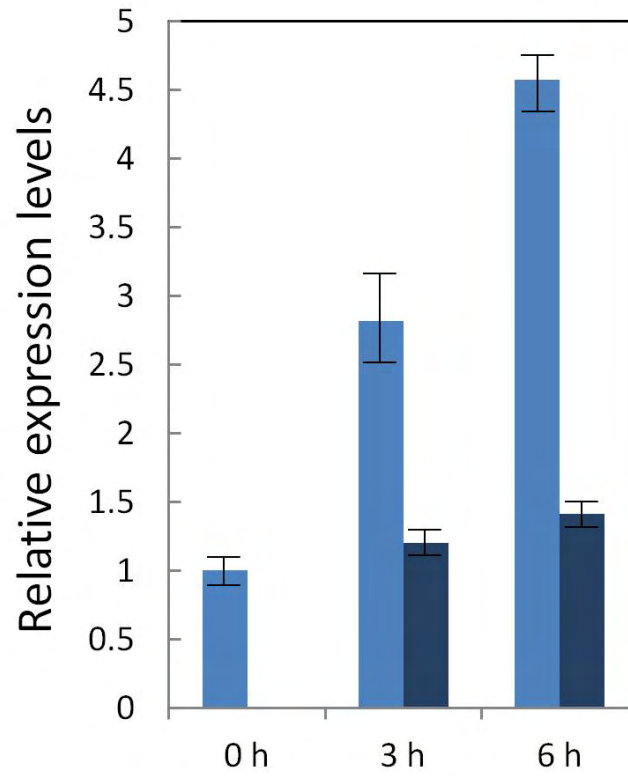


Fig. S4. Analysis of estrogen-inducible *LHW* plants. (A) Relative expression levels of *LHW* mRNA 0, 3 and 6 hours after the addition of estrogen (blue) and without estrogen (dark blue). Bars indicate s.d. (B,C) *DR5::GFP* signal in estrogen-inducible *LHW* roots 24 hours after the addition of estrogen (B) or DMSO (C).

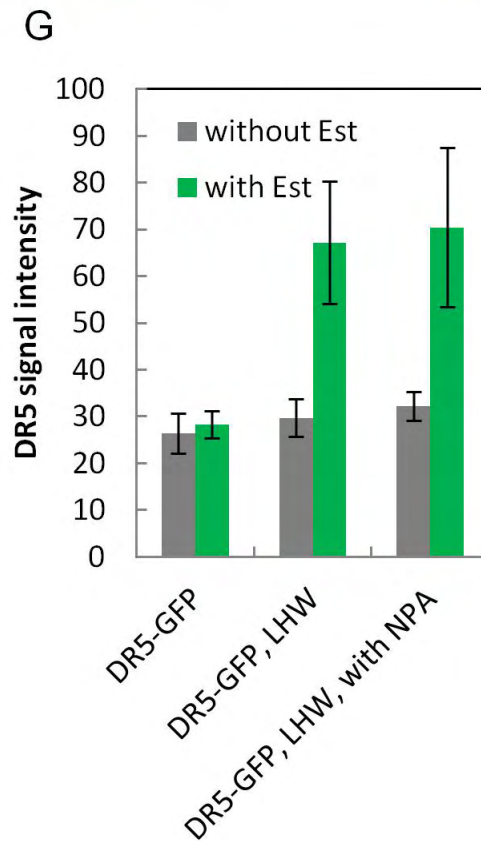
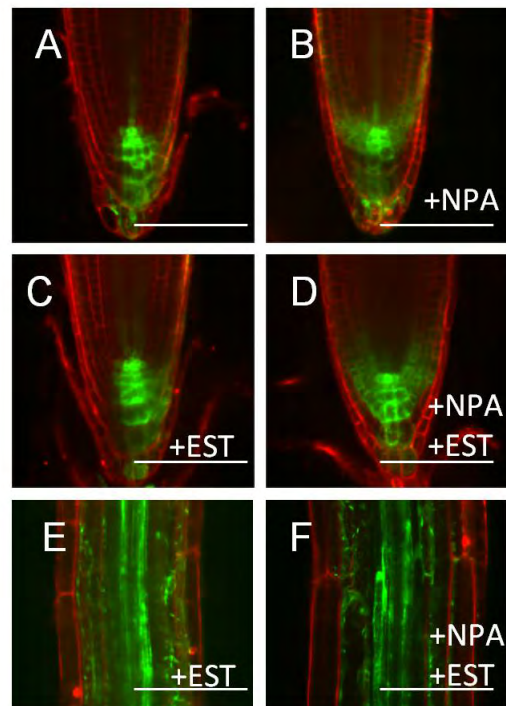


Fig. S5. Effects of NPA treatment on *DR5::GFP* expression. (A-F) *DR5::GFP* signal in estrogen-inducible *LHW* roots with or without NPA and estrogen. Images were taken 24 hours after these treatments. (G) *DR5::GFP* signal intensity in estrogen-inducible *LHW* plants with NPA treatment. *DR5::GFP* signal intensity in the differentiation zone of roots was measured at 24 hours after the induction of *LHW* with or without 10 μ M NPA.

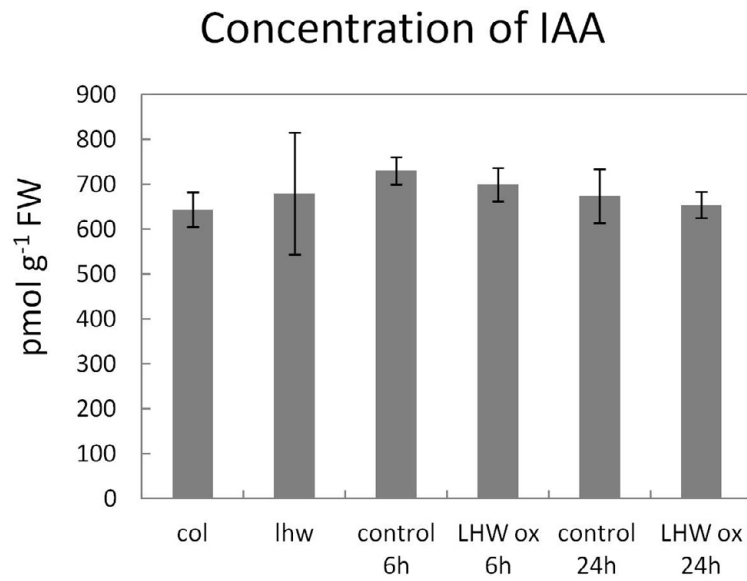


Fig. S6. Concentration of IAA in wild-type, *lhw* and *LHW*-overexpressing roots.

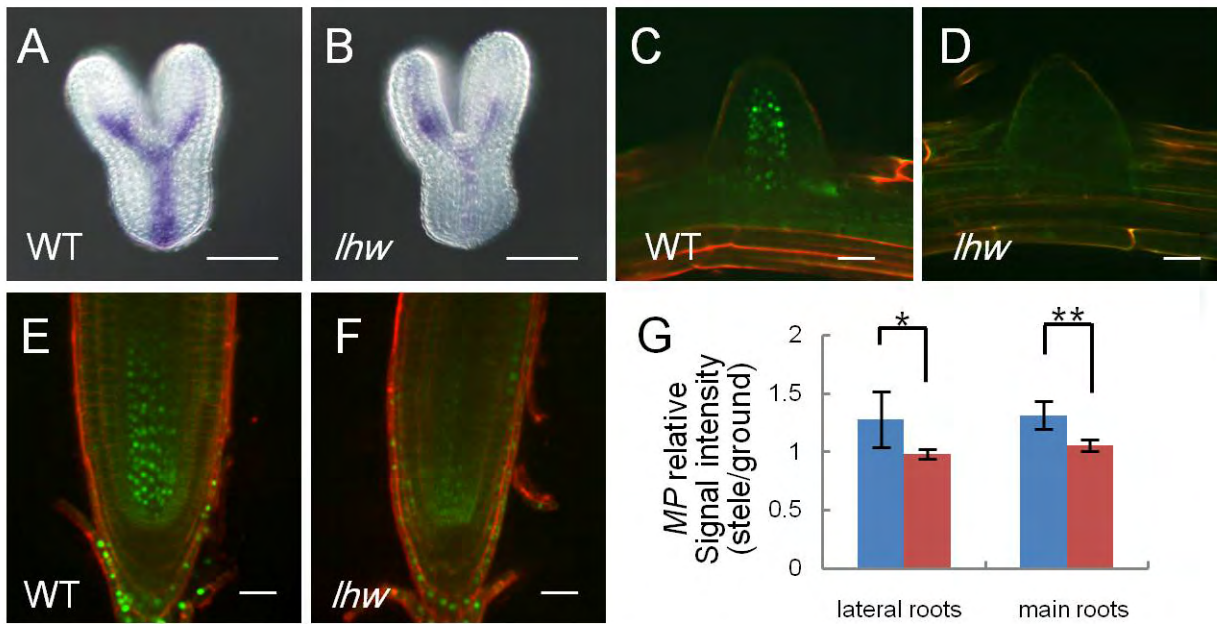


Fig. S7. LHW induces *MP* expression in the vascular region. (A,B) Whole-mount *in situ* hybridization using *MP* probe on wild-type (A) and *lhw* (B) embryos. (C,D) *MP::YFP-nls* expression in lateral root primordia of wild-type (C) and *lhw* (D). (E,F) *MP::YFP-nls* expression in root apical region of wild-type (E) and *lhw* (F). (G) Relative *MP::YFP-nls* signal intensity at stele versus ground tissue region in wild-type (blue) and *lhw* (red) roots. Bars indicate s.d. $n=5$, * $P<0.05$, ** $P<0.01$ (*t*-test). Scale bars: 50 μ m in A,B; 20 μ m in C-F.

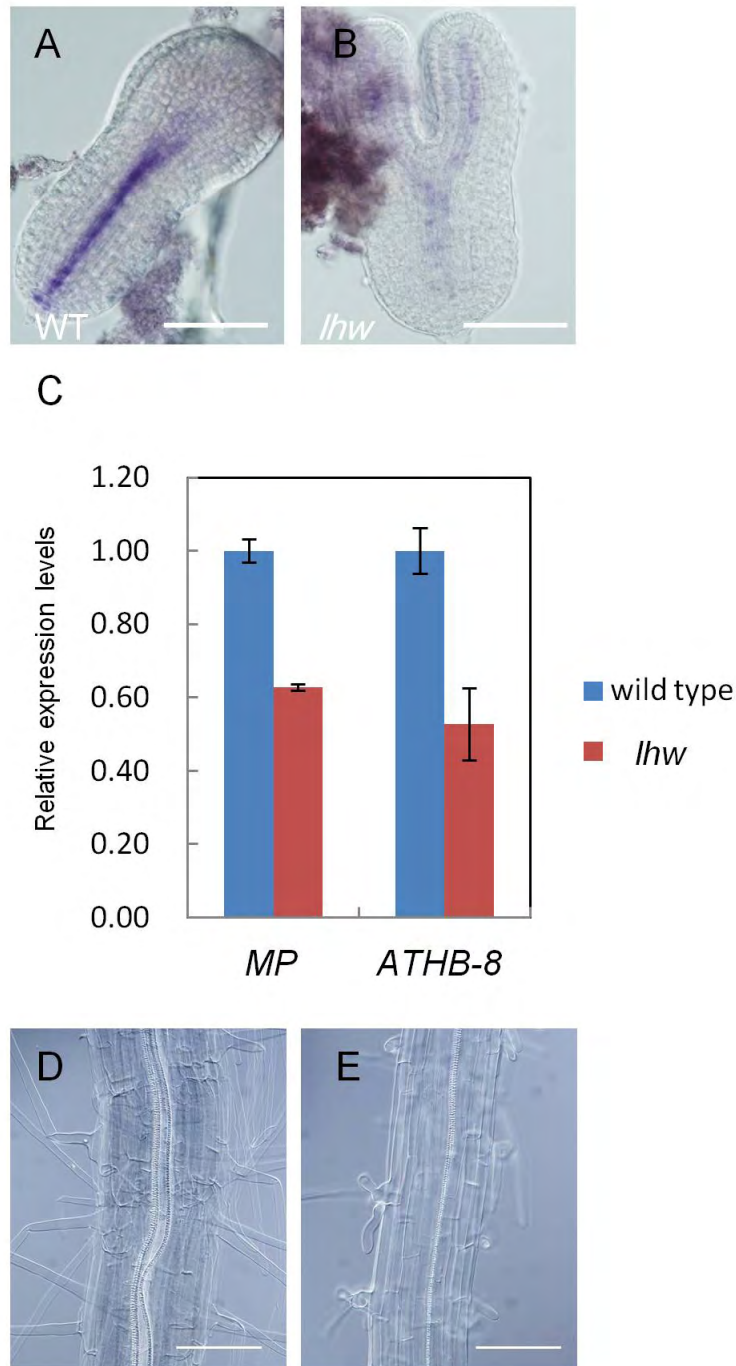


Fig. S8. Analysis of transcription factors related to auxin signalling. (A,B) mRNA accumulation patterns of *ATHB-8* in wild-type (A) and *lhw* (B) embryos. Scale bars: 50 μ m. (C) Quantitative RT-PCR of *MP* and *ATHB-8* transcripts. Total RNA isolated from wild-type and *lhw* roots was used for the analysis. Wild type (blue) and *lhw* (red). (D,E) DIC images of *lhw* roots harbouring *SHR::ATHB-8^r* (D) and *SHR::PHB^r* (E). Scale bars: 200 μ m.

Table S1. The list of primers used for this study

Purpose	Name	Sequences
RNA probe	LHW(1554)-F	GGAATCCAAGATTATGAAAGAGGACG
RNA probe	LHW-R1	TTACATTGAACAGCCACCAGTAAC
RNA probe	TMO5(651)-F	CTTGGTGATAAGAGCATCCTTTTGCT
RNA probe	TMO5-R	CTAATTATAACATCGATTACCATC
RNA probe	At1G68810(650)-F	ACATGTGAAAGAGTTGAAGAGA
RNA probe	AT1G68810-R	TTACCTCTGATTATATTGTTGTTG
RNA probe	MP-F	CACCATGATGGCTTCATTGTCTTGTG
RNA probe	MP-R	TTATGAAACAGAAGTCTTAAGATC
RNA probe	ATHB-8-F	ATGGGAGGAGGAAGCAATAATA
RNA probe	ATHB-8-R	TCATATAAAAGACCAGTTGAGG
qRT-PCR	LHW-real-F	AAACCGGGGAATCCAAGA
qRT-PCR	LHW-real-R	CCTACTTCGAAAGCCCATGT
qRT-PCR	MP-real-F	TGCCATATGCATCTTTCCTA
qRT-PCR	MP-real-R	GCCTCATCATCATTTTCATAAGC
qRT-PCR	ATHB-8-real-F	TGGGGCACTACCAAGAAGAC
qRT-PCR	ATHB-8-real-R	TGCACATTTGCAGAAGGAAG
qRT-PCR	MBF1A-real-F	TCGAGACCGTCAGAAAATTCA
qRT-PCR	MBF1A-real-R	CATTTTTGTGTTTCAGAGATGTGC
pAtPIN1	pPIN1(-1289)-F	CACCTCATTATATCATCAACCCATTG
	pPIN1(-5)-R	TGTTCCGCCGAGAAGAGA
pMP	pMP(-2050)-F	CACCGTATCCGAATAAGTAGTTATGTTTATATAGATATTCTATCATAAT
	pMP(-1)-R	CACCACAGAGAGATTTTCAATGTTCTGTTTGTCTCT
pSHR	pSHR(-2000)-F	CACCACATAAACCAGTAGACATATGGATAAATATGAACACA
	pSHR(-1)-R	CACCTTTTTTTTTTAAATGAATAAGAAAATGAATAGAAGAAAGGGAGAC
ATHB-8orf -mutagenesis	ATHB-8orf-SDM-F	TGGGTCCAAATGCCTGGGATGAAACCGGGGCCTGATTCCATAGGAATCG
	ATHB-8orf-SDM-R	CGATTCTATGGAATCAGGCCCCGGTTTCATCCCAGGCATTTGGACCCA
PHBorf -mutagenesis	PHBorf-SDM-F	TGGGTTTCAGATGATTGGGATGAAACCGGGGCCTGATTCTATTGGCATAG
	PHBorf-SDM-R	CTATGCCAATAGAATCAGGCCCCGGTTTCATCCCAATCATCTGAACCCA
pENTR-LHW	LHW-F	CACCATGGGAGTTTTACTAAGAGAAGCTT
	LHW-R	CACCATGGGAGTTTTACTAAGAGAAGCTT

Table S2. Quantification of phytohormones (pmol g⁻¹ FW)

	col	lhw	Control 6h	LHW _{ox} 6h	Control 24h	LHW _{ox} 24h
auxin						
IAA	643.67±39.05	680.29±135.9	730.56±30.25	699.55±37.05	673.91±59.75	654.13±29.42
IAAla	3.041±0.761	3.524±0.776	3.503±0.329	3.107±0.452	6.095±0.140	4.835±1.740
cytokinin						
tZ	0.549±0.168	0.743±0.095	0.864±0.093	0.691±0.063	0.950±0.116	1.348±0.302
tZR	1.753±0.091	4.395±1.006	2.273±0.165	2.506±0.426	3.257±0.538	6.015±0.111
tZRP _s	6.074±0.194	8.056±1.627	6.259±0.731	7.414±0.934	7.752±0.931	16.014±1.413
cZ	0.703±0.109	0.967±0.092	1.035±0.146	0.615±0.032	0.683±0.069	0.486±0.065
cZR	1.529±0.174	1.774±0.186	1.726±0.373	1.380±0.204	1.236±0.205	1.432±0.128
cZRP _s	4.154±0.435	4.335±0.861	3.982±0.985	3.336±1.166	2.296±0.188	3.394±0.507
iP	1.224±1.530	0.442±0.031	0.265±0.021	0.294±0.019	0.262±0.029	0.289±0.029
iPR	0.160±0.009	0.159±0.016	0.200±0.028	0.201±0.011	0.225±0.046	0.222±0.002
iPRP _s	8.864±0.193	10.804±0.340	7.245±1.890	9.631±1.587	8.584±0.788	9.940±0.334
tZ7G	2.940±0.146	3.452±0.237	5.905±0.434	5.989±0.515	6.421±1.367	5.525±0.205
tZ9G	2.812±0.165	3.327±0.108	4.698±0.232	4.919±0.212	5.387±0.751	4.659±0.129
tZOG	4.076±0.506	5.464±0.340	5.219±0.411	6.197±0.776	7.428±1.143	6.387±0.503
cZOG	2.971±0.181	4.501±0.064	2.340±0.298	2.716±0.201	2.628±0.321	1.895±0.148
tZROG	0.039±0.007	-	0.051±0.023	0.040±0.002	0.057±0.011	0.078±0.021
cZROG	0.164±0.048	0.264±0.073	0.184±0.033	0.188±0.022	0.193±0.025	0.224±0.018
iP7G	4.065±0.114	5.796±0.124	4.474±0.175	4.662±0.051	4.200±0.181	4.102±0.105
iP9G	0.905±0.085	1.448±0.058	0.889±0.058	0.894±0.030	0.862±0.104	0.815±0.082
others						
GA19	0.967±0.152	1.397±0.202	0.874±0.154	0.990±0.186	0.739±0.199	0.824±0.107
GA20	1.433±0.033	1.822±0.003	1.353±0.091	1.339±0.105	1.145±0.051	1.337±0.147
GA24	0.999±0.112	0.771±0.031	-	0.910±0.134	-	-
GA53	0.841±0.092	1.610±0.077	1.057±0.068	1.124±0.116	0.900±0.157	0.962±0.277
SA	12,355±71.69	19,778±2,400	29,806±14,511	23,794±3,475	26,853±6,758	23,367±2,692
JA	142.52±19.32	226.66±28.18	126.038±25.87	145.57±17.98	104.30±6.348	119.94±13.60
ABA	33.592±3.319	63.785±10.175	32.009±2.986	39.418±1.787	27.896±5.100	31.421±5.654

Concentrations of auxin, cytokinin, gibberellin, SA, JA and ABA in roots. Data are the means±s.d.

(n=3).